COMBINED CT AND MAGNETIC SCANNING TECHNIQUES FOR MULTIMODAL IMAGING OF FLUID FLOW IN POROUS MEDIA: APPLICATION TO HEAVY OIL WATERFLOODING

Petar Petrov[1], David K. Potter[1], Shauna Cameron[2], Mike London[2],
James Donald[2] and *Wade Waterman[2]
[1]Department of Physics, University of Alberta, Edmonton, Alberta, Canada
[2]Alberta Innovates - Technology Futures, Edmonton, Alberta, Canada

This paper was prepared for presentation at the International Symposium of the Society of Core Analysts held in St. John's, Newfoundland and Labrador, Canada, 16-21 August, 2015

ABSTRACT

Waterflooding is one oil recovery process used in heavy oil reservoirs. However, little has been published in terms of imaging heavy oil waterfloods, mainly due to the similar densities of water and heavy oil, which makes it difficult to track the advancement of the water/heavy oil front. The present study used computer tomography (CT) and magnetic susceptibility techniques to attempt to quantitatively image waterflooding of a heavy oil saturated sandpack, and monitor the progress of the water/heavy oil front in real time. A low concentration of superparamagnetic nanoparticles (20 nm diameter maghemite) was added to water during the flooding. These particles act as dual response contrast agents, having an extremely high magnetic susceptibility that can be monitored magnetically via a surrounding sensor, and an increased X-ray attenuation over water alone for CT scanning. Jar tests were first undertaken to establish the optimum conditions for both CT and magnetic susceptibility scanning.

Waterflooding, with the dilute nanoparticle suspension, of a heavy oil saturated sandpack revealed the formation, growth and movement of a significant positive magnetic susceptibility peak. This formed at the injection end of the flow cell and migrated towards the production end as the waterflooding progressed. The peak was likely due to a higher concentration of nanoparticles collecting at the main water/heavy oil front. This appears to provide a means of quantitatively tracking the position of the front in real time. The increased accumulation of nanoparticles at the main front was further supported by material collected in the production jars. Whilst the CT attenuation profiles in part of the sandpack showed some correspondence with the magnetic results, the CT profiles did not show a recognizable front. This may be due to the low contrast between the water + nanoparticles and the heavy oil, to the presence of trapped gas, and to the shallow and diffuse nature of the front in a waterflood with heavy oil. Once the main water/heavy oil front had passed through the sandpack the magnetic profiles had a constant shape similar to the porosity profile (confirmed by the CT derived porosity variation). The magnetic technique has potential for monitoring larger scale commercial waterflooding operations.

INTRODUCTION

There is little in the literature regarding quantitatively imaging waterflooding of a heavy oil saturated sandpack (simulating one of the oil recovery processes employed in the oilsands of Northern Alberta and elsewhere), although there are related studies on viscous fingering [1] and using CT scanning of waterflooding in low permeability chalk [2]. The main aim of this project was to provide a means of quantitatively imaging the waterflooding of a heavy oil saturated sandpack, and tracking the water / heavy oil front in real time. Monitoring such waterflooding using CT scanning, without the addition of a contrast agent, is very difficult due to the similar densities of water (1.00 g/cc) and heavy oil (0.99 g/cc). Therefore it was proposed that the addition of superparamagnetic nanoparticles to the water (or brine) phase might improve the CT contrast between the water (or brine) phase and the heavy oil. Moreover, these nanoparticles would act as dual contrast agents, and their progress can be also be independently monitored by a magnetic susceptibility sensor [3]. The advantage of the nanoparticles is that they have an enormously higher magnetic susceptibility compared to the sandpack, the water or the heavy oil. The sandpack (quartz) and fluids are dominantly diamagnetic, which means they have very low negative values (quartz theoretically has a mass magnetic susceptibility of -0.62×10^{-8} m^3 kg^{-1} and the magnetic susceptibility of typical reservoir fluids is given in [4]). The superparamagnetic maghemite nanoparticles, on the other hand, have a value around $55{,}000 \times 10^{-8}$ m^3 kg^{-1} (which varies a bit depending upon how they are dispersed). A series of jar tests (without porous media) were initially conducted in order to identify the most appropriate nanoparticles for both CT and magnetic use, and to determine the optimum conditions for their dispersion and stability over prolonged time periods in water and various brines. A waterflooding experiment was then undertaken on a heavy oil saturated sandpack to evaluate the effectiveness of the nanoparticle injection for the CT and magnetic scanning techniques.

METHODS

Jar Tests Prior to Waterflood Experiment

A series of superparamagnetic nanoparticle dispersions (testing maghemite, magnetite and nickel ferrite nanoparticles) were first prepared for magnetic susceptibility scanning and CT scanning jar tests without porous media. We prepared brine samples where the nanoparticles were dispersed in sodium chloride or in sodium iodide. In each case a small amount of dispersant, sodium dodecylbenzeno sulfonate (DDBS), was added to each sample. This was followed by sonication for several minutes. Tests had shown that this anionic dispersant (rather than a cationic dispersant such as cetyltrimethyl ammonium bromide), followed by sonication, was the most effective way of dispersing the nanoparticles. The maghemite nanoparticles remained in suspension longer than the other types, and were thus chosen for the subsequent waterflood experiment. Nevertheless, these maghemite nanoparticles still tended to settle out in a timescale of around 1 hour. CT contrast tests indicated that there could potentially be enough X-ray contrast to observe a waterflood with any of the nanoparticles, but that the variability of measured values, combined with the expected porosity and saturation contrast, made such a

conclusion uncertain. Substituting iodine for chlorine in the brine enhanced the oil-brine contrast.

A second set of jar tests were carried out to determine the optimum conditions required for creating long term stable maghemite nanoparticle suspensions. The stability with time of different solution compositions (nanoparticle, DDBS dispersant, sodium iodide and sodium chloride concentrations), as well as different mixing processes (mechanical and sonication), was determined using a Bartington MS2C sensor. The jar tests revealed that the addition of sodium iodide or sodium chloride, either before or after the formation of the suspension, caused the nanoparticles to agglomerate and settle out relatively fast. The jar tests composed of only nanoparticles and DDBS dispersant mixed in deionised water displayed remarkable stability over long periods of time, consistent with our previous stability and flow experiments [3]. Therefore we decided to use deionised water rather than brine in the waterflood experiment, and the CT contrast would be provided by the nanoparticles themselves.

Experimental Set-up for Waterflood Experiment

A PEEK flow cell was assembled and leak tested in preparation for the waterflood experiment. We used a Hassler-type vessel with a confining pressure (radial) of 600 kPa during the waterflooding. A Viton sleeve was packed with around 78 g of sand and then inserted into the flow cell. The sandpack was 114.3 mm long and approximately 22.2 mm in diameter. The core material is water wet Ottawa sand, F110 from the U.S. Silica Company. F110 is a pure quartz sand (99.8% SiO_2) with minor amounts of Fe_2O_3, Al_2O_3 (<0.1% each), and other oxides. Grain diameter is 50–150 μm. Particles are subangular, and the size distribution is as follows: 8% 53–75 μm, 25% 75–106 μm, 44% 106–150 μm, 18% 150–212 μm, and 4% 150–212 μm, with <1% beyond the upper and lower limits. The median particle diameter is 85 μm, the median pore diameter 46 μm, and the median throat diameter 18 μm. The absolute permeability was estimated to be 5 Darcy. Dry CT scans were performed as a baseline measure at 135 kVp and 100 mA with an Aquilion One CT scanner. All CT scans for the remainder of the experiment, were collected at these settings. The experimental setup of the flow cell, magnetic susceptibility sensor and CT scanner for the waterflood experiment is shown in **Figures 1 and 2**. A Bartington MS2C coil magnetic susceptibility sensor, connected to an MS2 meter, surrounded the flow cell. The coil sensor could be moved so as to make measurements at any desired point along the flow cell. The majority of the magnetic susceptibility signal is contained within a thin disc-shaped slice approximately 16 mm wide, 8 mm either side of the measure point (the centre of the plane of the sensor coil). New non-metallic (PEEK) end fittings were manufactured for the flow cell, which reduced the background noise signal during the magnetic susceptibility measurements. The flow cell assembly was modified so that the magnetic sensor could be removed after each CT scan, allowing the re-zeroing of the magnetic sensor prior to each magnetic scanning sequence.

Table 1 summarises the main conditions of the waterflood experiment. Two pore volumes (PV) of deionised water were first injected into the sandpack at approximately 60 mL/hour. Each pore volume was approximately 15 cc. CT scans were again performed at this stage for baseline values. The MS2C magnetic sensor was also employed to gather baseline readings at this stage. Measurements were taken every 0.5 cm along the 15 cm length of the sandpack within the vessel. An oil flood, using Lloydminster heavy oil of 20,000 cP viscosity, was then undertaken at an average flow rate of approximately 0.5 mL/hour for 1.2 pore volumes, followed by a set of baseline oil CT scans and a set of MS2C magnetic sensor measurements. The oil flood is a kind of Swi setting.

Table 1. Summary of the main conditions of the waterflood experiment.

Conditions for Waterflood Experiment	
Heavy oil saturation:	
Injection rate	0.5 mL/hr
Total injected	1.2 PV
Waterfloods:	
Maghemite nanoparticle concentration	0.6 wt %
DDBS concentration	0.81 wt %
Sonication	20 min
Sodium iodide	none
FLOPAAM	none
Shaker for accumulator	no
Injection rate	1 mL/hr
Breakthrough (produced) volume	0.04 PV
Total deionised water injected	1.75 PV
Total oil produced	0.2 PV

For the waterflood, maghemite nanoparticles were added to deionised water at 0.6 wt% (**Table 1**) and mechanically agitated. The dispersing surfactant sodium dodecylbenzenesulfonate (DDBS) was then added at a concentration of 0.81 wt%. The solution was mechanically agitated and sonicated for 20 minutes in an ice bath prior to injection into the sandpack. The target injection rate was 1 mL/hour for the duration of the experiment. A total of 1.75 pore volumes of solution were injected into the sandpack and 13 sets of CT scans and magnetic sensor measurements were collected at regular intervals during injection. The nanoparticle tracer is not expected to go into the oil. One Dean Stark test was performed post experiment to determine oil, water, and solids.

RESULTS AND DISCUSSION

Figure 3 shows the produced oil versus the injected water during the waterflood. **Figure 4** shows a few smoothed CT attenuation profiles of differences from the oil saturated scan for the first 60mm of the sandpack, and **Figure 5** shows the final change from the oil

saturated state for the entire length of the sandpack. The vertical scale on **Figure 4** has been expanded to show the differences. Based on the calibrated nanoparticle-oil contrast of 24 Hounsfield units (HU) and a porosity of about 1/3, the peak value of 4 HU corresponds to an increase in saturation of 50%. The CT profiles clearly showed an increase in the attenuation between profiles 1 and 7 consistent with an increased magnetic susceptibility (due to injection of nanoparticles) as shown in **Figure 6**. Moreover, the CT attenuation dropped once the main front (identified from the magnetic susceptibility results and the material collected in the production jars) passed through the sandpack, consistent with the magnetic susceptibility profiles of **Figure 7**. However, the CT profiles did not exhibit a clearly recognisable front to the waterflood (neither did an earlier waterflood experiment using a sodium iodide solution). The CT profiles also showed a region of high attenuation (a "hump" at 70-80 mm from the inlet) followed by low attenuation in the downstream part of the sandpack (**Error! Reference source not found.**). The latter prevented any meaningful calculation of saturation profiles downstream of the hump. The low attenuation may have been caused by gas that was trapped in the pack during the initial water saturation and not fully swept out by the oil saturation. The CT attenuation responds to the nanoparticles and the fluids, including any trapped gas. The origin of the hump feature is unclear at present. It remained in the same position in each CT profile and did not appear to correlate with the magnetic susceptibility peak (**Figure 6**) which evolved and moved during the waterflooding as detailed below.

Eight volume magnetic susceptibility profiles were measured during the first day of nano-fluid injection (Error! Reference source not found.**6** shows profiles 3-8). The points on the profiles directly represent the content of maghemite nanoparticles at each point in the sandpack along the flow cell. The profiles revealed the progressive formation, growth and movement of a significant positive magnetic susceptibility peak, which initially formed on the left injection side of the flow cell (Error! Reference source not found.**6**, profiles 3 and 5) and migrated towards the right production (outlet) side as the injected volume of nanoparticle suspension increased (Error! Reference source not found.**6**, profiles 6-8). The peak is likely the result of a higher concentration of nanoparticles collecting at the site of the main water-heavy oil front during the flooding process. The peak may not necessarily reflect a higher water saturation at the peak (compared to portions of the sandpack closer to the inlet), since it appears that the nanoparticles agglomerate at the front (from material collected in the production jars as discussed later). First breakthrough (nano-fluid recovered at the production end) was observed after an injection of approximately 8.46 ml (0.2 PV injected or 0.04 PV produced) halfway between profiles 5 and 6. This is consistent with the observed magnetic susceptibility profiles. Profile 5 shows negative magnetic susceptibility at the production end (right side of the graph) indicative of the absence of nanoparticles, while profile 6 has a clear positive magnetic susceptibility signal on the production end, which can only occur if nanoparticles are flowing through that section. Therefore it appears that breakthrough of the nanoparticle suspension occurred before the main front, whose progress was tracked by the magnetic susceptibility peak, reached the production end. This may happen if, for

instance, viscous fingering is occurring. The results of Error! Reference source not found.**6** show how magnetic sensing of a nanoparticle suspension can track the progress of the main front during water flooding of a heavy oil saturated sandpack. This would appear to be a significant result. The shape of the front is likely to be complex, but the overall position of the main front appears to be tracked by the peak in magnetic susceptibility in each of the curves of **Figure 6**. The physical mechanism as to why the nanoparticles agglomerate at the front is not completely understood at present. A review of processes affecting nanoparticles at fluid interfaces is given by Bresme and Oettel [5]. In our case we think it may be due to a weakening of the repulsive electrical double layer around the nanoparticles, making them more likely to agglomerate. One possible cause of the weakening of the electrical double layer could be due to adsorption of hydroxyl ions at oil-water interfaces as described by Marinova et al. [6].

After the main front had passed through the production end of the flow cell the magnetic profiles of Error! Reference source not found.**7**, taken on the second day, show that the maximum magnetic susceptibility was lower than the peak observed in Error! Reference source not found.**6**. This would be expected if nanoparticles are no longer collecting at a major front. The magnetic profiles shown in Error! Reference source not found.**7** also had a relatively constant shape, which was expected to reflect the porosity profile. Higher porosity areas should give larger magnetic signals due to the higher volume of nanoparticles. CT scanning (Error! Reference source not found.**8**) confirmed that the porosity profile was very similar to the magnetic profiles. In particular, the decrease in magnetic susceptibility (Error! Reference source not found.**7**) just before 60 mm from the inlet end seems to correspond with a similar decrease in the CT porosity profile (Error! Reference source not found.**8**). There is also a correspondence because the Sor value is quite homogeneous within the sandpack because the brine volume measured is locally a function of phi*(1-Sorw) and not phi only. Note that the magnetic and CT values are the result of different “thickness slices” at each point (16 mm for the magnetics versus 0.35 mm for the CT), and this might explain differences between the two types of profile. Note also that the magnetic susceptibility values decrease slightly at both the inlet and outlet ends of the flow cell because the sensor is sensing outside the region of the sandpack at these points. **Figure 7** also indicates that there were slight increases in magnetic susceptibility with time. This is likely due to an increase in the volume of magnetic nanoparticles within the pore spaces, as nano-fluid was continuously displacing the oil.

The growth and migration of the magnetic susceptibility peak shown in Error! Reference source not found.**6** strongly suggests that the nanoparticles accumulated at the main front. This was further supported by observations of the material in the production jars (Error! Reference source not found.**9**). The production jar relating to the main front (JAR #5) contained nanoparticle agglomerates that had settled out of suspension. Such agglomerates were not subsequently seen in the later production jars after the main front had passed through the production end. These later jars (JARS #6 and #7) had nanoparticles still in suspension.

CONCLUSIONS

1. The formation, growth and movement of a magnetic susceptibility peak during the waterflood is consistent with a higher concentration of nanoparticles collecting at the site of the main front during the flooding process. This appears to provide a means of quantitatively tracking the progression of the front in real time. The aggregation of the nanoparticles at the front, however, may mean that the magnetic susceptibility values might not quantitatively relate to the water saturation as the front is passing through the sandpack.
2. Further independent evidence for a higher concentration of nanoparticles accumulating at the main front was provided by the material collected in the production jars.
3. Once the main water/heavy oil front had passed through the production end of the flow cell the magnetic profiles had a relatively constant shape, which reflected the porosity profile of the sandpack as confirmed by the CT results. After the main front has passed through the sandpack the magnetic results should potentially provide a quantitative measure of water saturation, since the nanoparticles were dispersed and in suspension at this stage (as seen from the material collected in the production jars) similar to the originally injected nano-fluid.
4. The CT attenuation profiles do not presently show a recognizable front. Part of the reason for this could be the relatively low contrast between the water + nanoparticles and the heavy oil, whereas for the magnetic results there is a substantially larger contrast between the magnetic susceptibility of the nanoparticles and that of the sandpack or fluids. It may also be due to the smallness of the change in saturation that the front represents. In addition, the CT attenuation results appear to have been corrupted by trapped gas in the downstream part of the sandpack.

ACKNOWLEDGEMENTS

We thank Alberta Innovates - Technology Futures (AITF) for funding for this project, in particular Marlene Huerta of AITF for all her support.

REFERENCES

1. Da Costa e Silva, A. (1995). Analysis of viscous fingering reproducibility in consolidated natural porous media. *Society of Core Analysts conference*, Paper Number 9504, pp. 1–10.
2. Mogensen, K., Stenby, E. H., & Zhou, D. (2001). Studies of waterflooding in low-permeable chalk by use of X-ray CT scanning. *Journal of Petroleum Science and Engineering*, **32**, 1–10.

3. Khan, S., Potter, D. K. & Kuru, E. (2015). Quantifying the transport of superparamagnetic nanoparticles in porous media using an acrylic flow cell and integrated magnetic susceptibility sensor technique. *Transport in Porous Media*, **106** (issue 3), 691-705.
4. Ivakhnenko, O. P. and Potter, D. K. (2004). Magnetic susceptibility of petroleum reservoir fluids. *Physics and Chemistry of the Earth*, **29**, 899-907.
5. Bresme, F. and Oettel, M. (2007). Nanoparticles at fluid interfaces. *Journal of Physics: Condensed Matter*, 19 (issue 41), Article Number 413101 (33pp). DOI: 10.1088/0953-8984/19/41/413101.
6. Marinova, K. G., Alargova, R. G., Dencov, N. D., Velev, O. D., Petsev, D. N., Ivanov, I. B. & Borwankar, R. P. (1996). Charging of oil-water interfaces due to spontaneous adsorption of hydroxyl ions. *Langmiur*, **12**, 2045-2051.

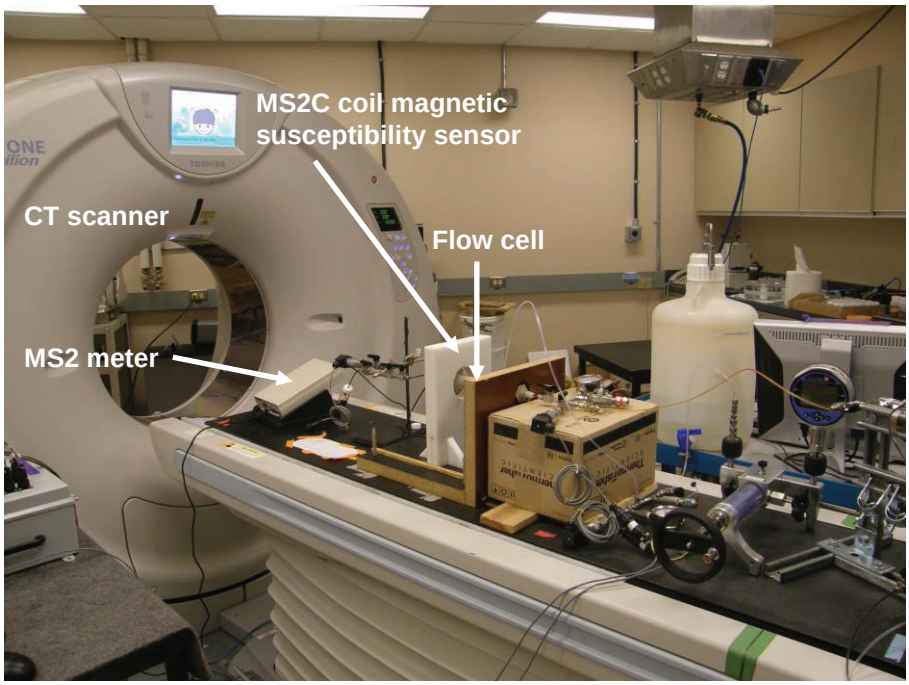

Figure 1. The experimental setup on the CT couch for the waterflood experiment, with the flow cell and magnetic sensor in place.

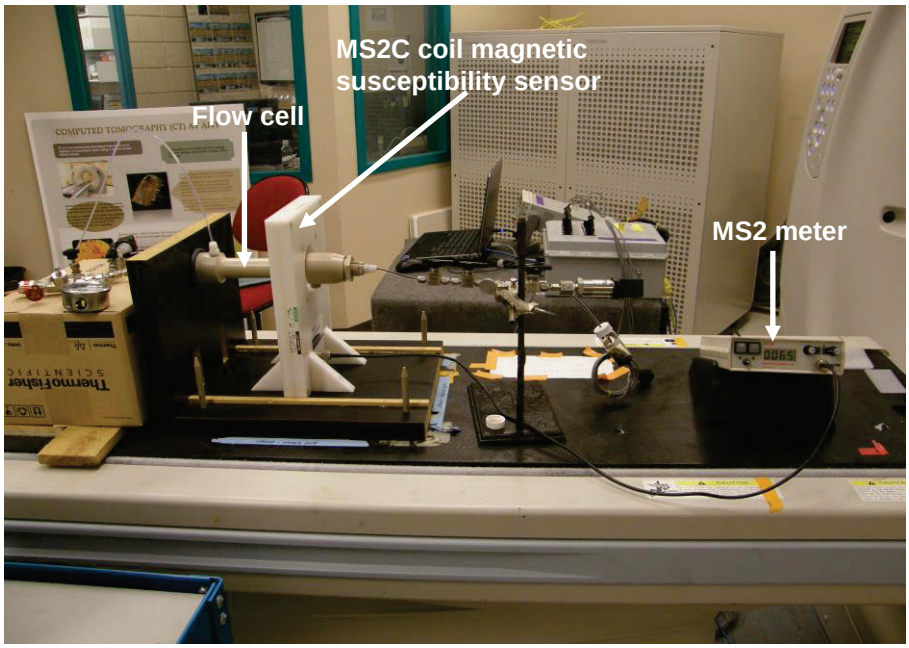

Figure 2. Close up of the flow cell and magnetic sensor on the CT couch for the waterflood experiment. Water injection is from left to right.

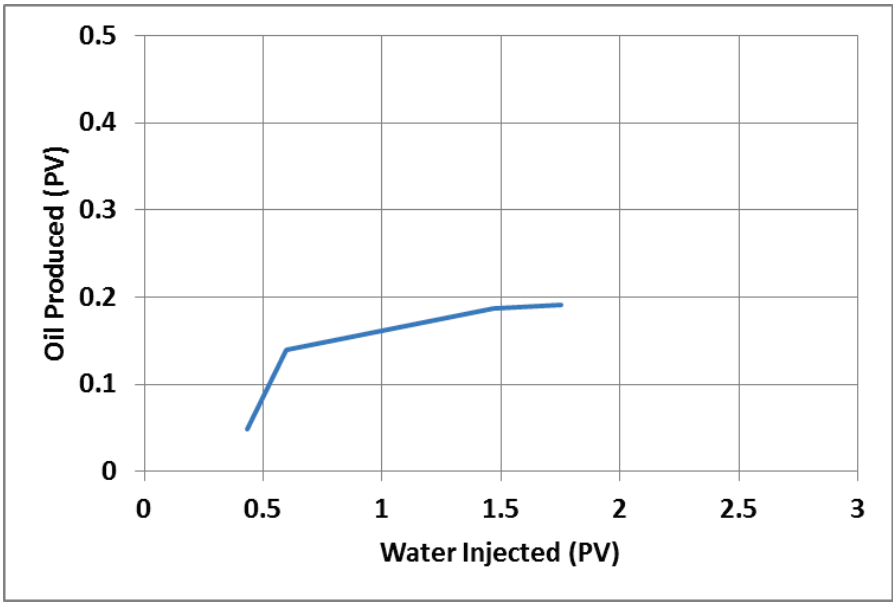

Figure 3. Produced oil versus injected water during the waterflood. Breakthrough occurred at about 0.04 PV produced or 0.2 PV injected. This was observed before the first production jar was removed, therefore before the first point on the production curve in **Figure 3**. Before and after breakthrough, production behaved as if there were compressible fluid present. Our analysis of the pressure drop across the pack suggests between 0 and 1 ml of gas (depending on where it may have been lodged) trapped in the pack. The rest (accounting for the discrepancy between injected and produced volumes) could have been in either the production or the injection plumbing (or both).

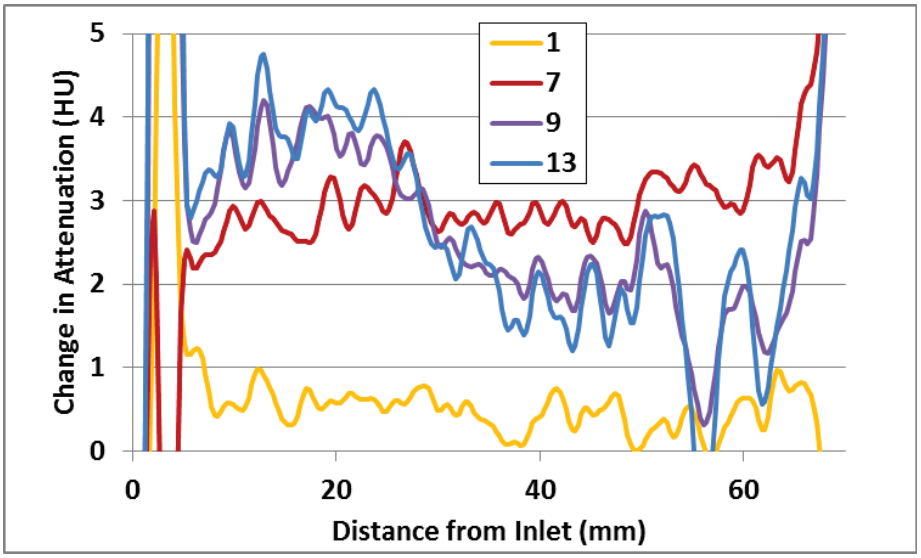

Figure 4. CT attenuation profiles for the upstream portion of the sandpack. Attenuation values are given in Hounsfield units (HU). Profile 13 was taken about a day after profile 1. Injection is from left to right.

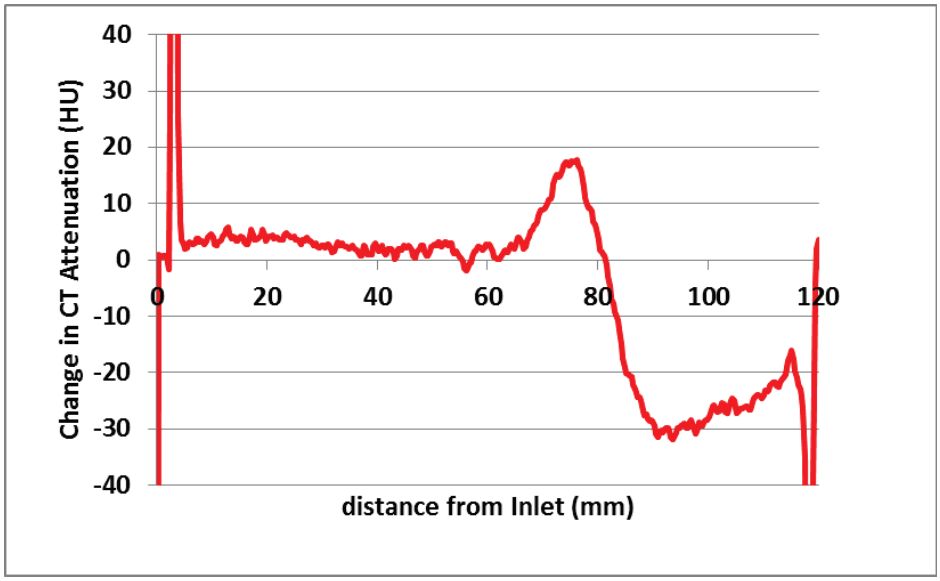

Figure 5. Final change in attenuation from the oil saturated scans observed in the medical CT scanner after 1.75 pore volumes of water + dispersed nanoparticles were injected into the heavy oil saturated sandpack. The figure shows a small increase in attenuation in the first 60 mm, due mainly to the nanoparticles. The

features beyond 60 mm appear to be artefacts. The hump feature at 70-80 mm is presently unexplained, but does not correlate with the magnetics. The low attenuation beyond 80 mm appears to be due to trapped gas.

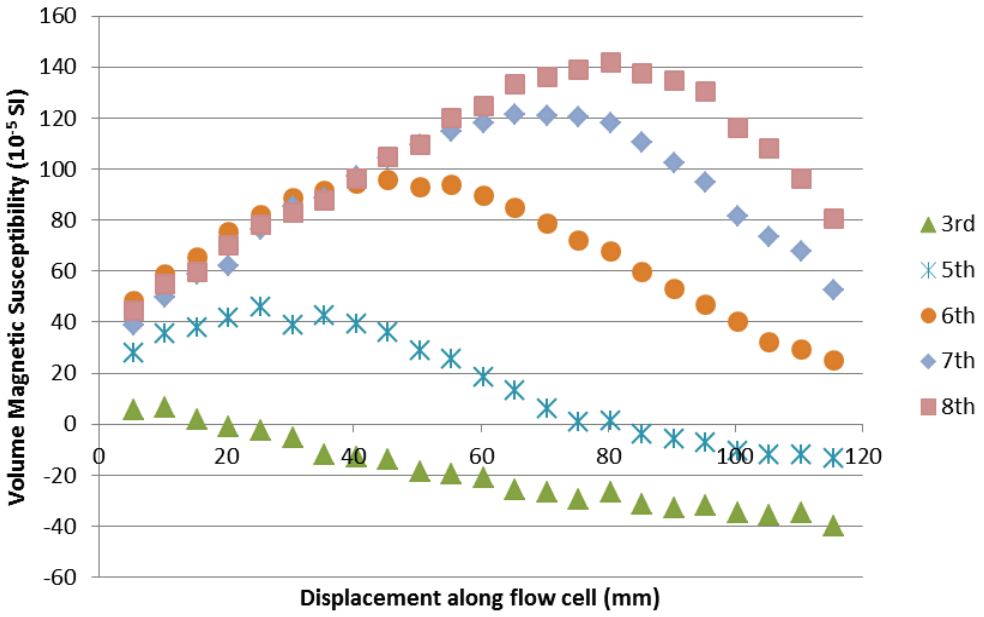

Figure 6. Volume magnetic susceptibility profiles taken during day one of the nano-fluid flooding of a heavy oil saturated sandpack.

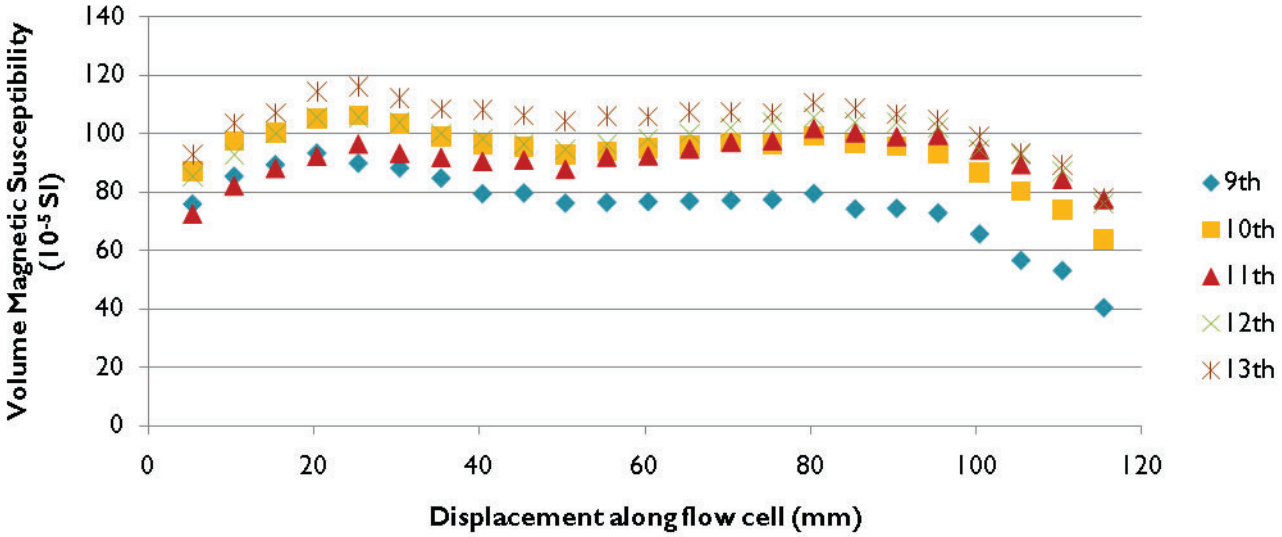

Figure 7. Volume magnetic susceptibility profiles taken during day two of the nano-fluid flooding.

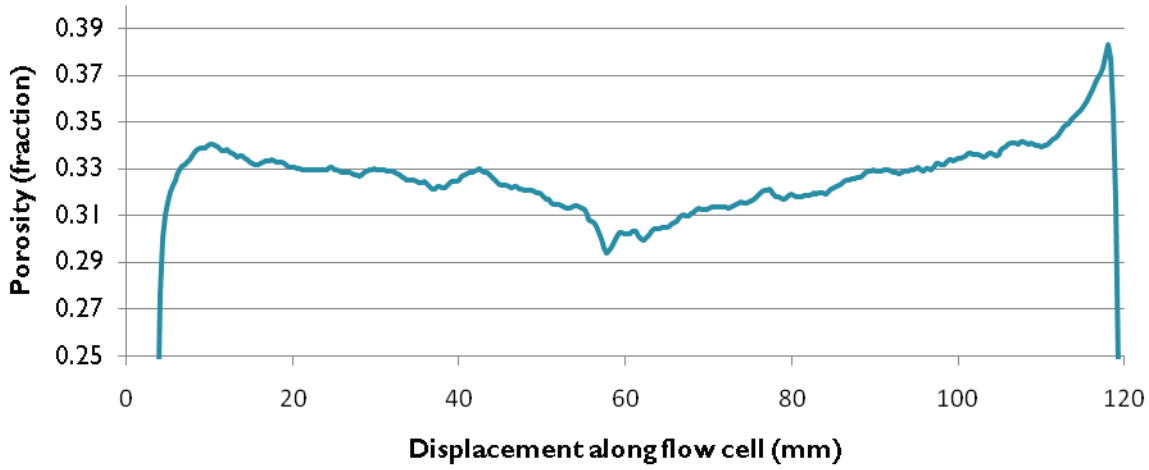

Figure 8. CT scanning porosity profile of the sandpacked flow cell. Note the overall similar shape to the magnetic susceptibility profiles in **Figure 7**.

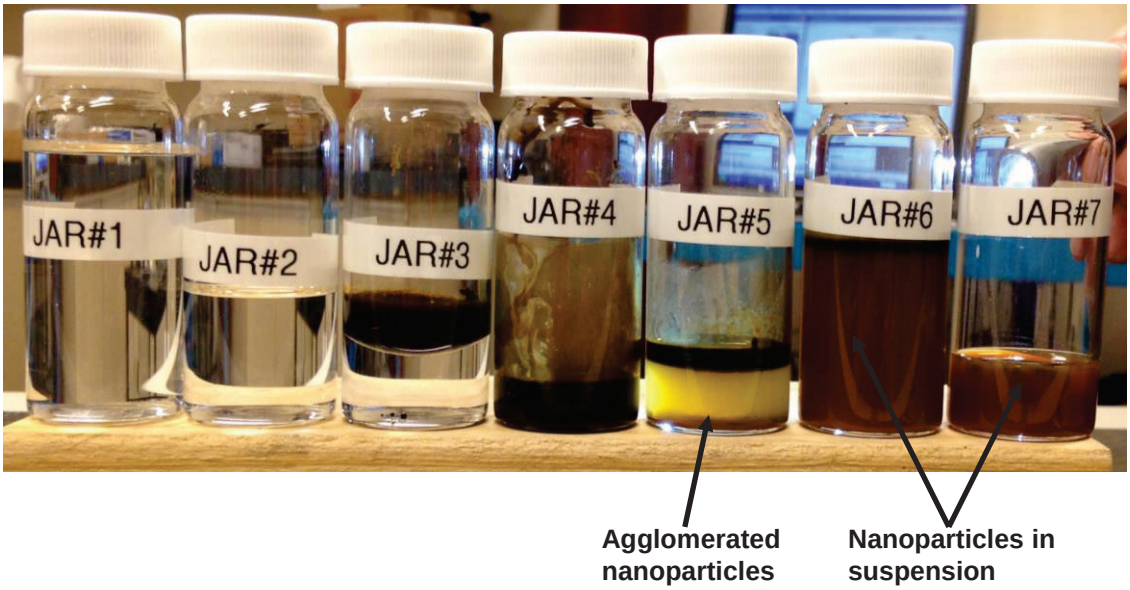

Figure 9. Production jars from the waterflood experiment: initial waterflood JAR #1, oil flood JARS #2 and #3, nanoparticle suspension flood JARS #4 to #7. Production JAR #5 clearly shows that nanoparticles have agglomerated and come out of suspension (lower thin brown layer). Above this is a yellow layer which comprises water plus some nanoparticles, and this is overlain by a heavy oil layer (black layer). The later production JARS #6 and #7 clearly show nanoparticles in suspension and not separated out.